CIRRELT

CIRRELT-2025-17

Tactical Network Planning for Intermodal Barge Transportation Considering Varying Water Levels

Bita Payami
Ioana C. Bilegan
Teodor Gabriel Crainic
Walter Rei

May 2025

Bureau de Montréal
Université de Montréal
C.P. 6128, succ. Centre-Ville
Montréal (Québec) H3C 3J7
Tél : 1-514-343-7575
Télécopie : 1-514-343-7121

Bureau de Québec
Université Laval,
2325, rue de la Terrasse
Pavillon Palasis-Prince, local 2415
Québec (Québec) G1V 0A6
Tél : 1-418-656-2073
Télécopie : 1-418-656-2624

Tactical Network Planning for Intermodal Barge Transportation Considering Varying Water Levels

Bita Payami[1], Ioana C. Bilegan[2], Teodor Gabriel Crainic[1,*], Walter Rei[1]

1. Interuniversity Research Centre on Enterprise Networks, Logistics and Transportation (CIRRELT), School of Management, Université du Québec à Montréal
2. Univ. Polytechnique Hauts-de-France, LAMIH, CNRS, UMR 8201, F-59313 Valenciennes, France

Abstract. Barge transportation provides a sustainable and cost-effective alternative to road transport, offering solutions to reduce congestion and lower emissions. However, increasing drought frequency and severity, driven by climate change, along with human interventions such as dam operations, dredging, and water withdrawals, cause fluctuations in water levels in rivers and canals that jeopardize its reliability and efficiency. These variations, including shallow water conditions, reduced water levels, and restricted navigable depths, directly impact barge operations by limiting transportation capacity. A barge's load capacity depends not only on its physical characteristics but also on the available water level along its route. Insufficient or diminished water levels impose draught restrictions that constrain freight volume and weight, creating operational challenges that hinder carriers' ability to meet shipper demands efficiently and maintain profitability. This study presents a tactical planning framework for consolidation-based barge transportation that explicitly models the relationship between water levels and barge load capacity. The framework integrates vessel characteristics and predicted water levels to optimize resource utilization and maximize expected carrier revenue while ensuring reliable demand fulfillment. Through computational experiments conducted using a commercial software, we analyze how varying water levels in rivers and canals impact profitability, operational efficiency, shipper satisfaction, and the service network structure.

Keywords: Barge transportation, water level fluctuations, tactical planning, service network design, consolidation-based transportation

Acknowledgments: While working on the project, the first author was Ph.D. candidate at the School of Management, Université du Québec à Montréal (UQAM), Canada, and member of CIRRELT. The third author held the UQAM Chair in Intelligent Logistics and Transportation Systems Planning, and was Adjunct Professor in the Department of Computer Science and Operations Research at the Université de Montréal, while the fourth author held the Canada Research Chair in Stochastic Optimization of Transport and Logistics Systems. We gratefully acknowledge the financial support provided by the Natural Sciences and Engineering Research Council of Canada (NSERC), through its Collaborative Research and Development, and Discovery grant programs. We also gratefully acknowledge the support of Fonds de recherche du Québec through their infrastructure grants. Finally, during the preparation of this work the authors used ChatGPT-4, under its most strict privacy enforcing settings, for text edit purposes exclusively. After using this tool, the authors reviewed and further edited the text as needed and take full responsibility for the content of the publication.

---

* Corresponding author:teodorgabriel.crainic@cirrelt.net

Dépôt légal – Bibliothèque et Archives nationales du Québec
Bibliothèque et Archives Canada, 2025

1 Introduction

Inland waterways, including rivers and canals, are crucial for freight transport. In the United States, they handled approximately 495 billion tonne-kilometers of cargo annually from 2004 to 2022 (CEIC Data , 2023). Similarly, European Union (EU) waterways transported 469 million tons of goods in 2023 (Eurostat , 2023). Globally, barges play a critical role in regions with extensive waterway networks, offering a highly efficient and environmentally sustainable mode of transportation. A single barge can replace 40 to 60 trucks, reducing fuel consumption by 75% and greenhouse gas emissions by 80% compared to road transport. Barges also require significantly less energy per ton-kilometer, consuming only 17% of road transport energy and 50% of rail transport energy. Due to these advantages, barges are increasingly integrated into intermodal freight transportation systems, where different modes—such as barges, trucks, trains, and airplanes-are integrated to form an efficient and flexible transportation network. This integration is particularly advantageous in regions with well-developed inland waterway infrastructure.

Within these systems, consolidation-based inland waterway carriers operate scheduled services across terminals connected by navigable waterways. Each service is operated by a vessel and follows a fixed route—including origin, destination, and potentially intermediate stops—with specified departure and arrival times. It is characterized by the vessel's physical attributes (e.g., draught, length, load capacity) and operational features (e.g., speed, cost). Carriers offer these services in response to transportation demands from shippers, who request that shipments be picked up from the origin terminal no earlier than their availability time and delivered to the destination terminal no later than the due time, often with specific service quality requirements (e.g., standard or express). A key challenge in this context is tactical planning, which involves jointly selecting a cost-efficient set of services and schedules while optimizing shipment itineraries that define routing and operations (e.g., transfers, consolidation). (Bilegan et al. , 2022) provide an in-depth discussion of tactical planning in intermodal freight transportation for inland waterway transport (IWT) carriers. They propose a new Scheduled Service Network Design model with integrated Resource and Revenue Management (SSND-RRM) to optimize service schedules, resource utilization, and shipment routing, aiming to maximize carriers' revenues while accommodating diverse shipper categories and service quality requirements.

The current study contributes to the literature by incorporating the effects of water level variability into an SSND-RRM formulation—an environmental and infrastructure constraint that directly influences vessel operability and load capacity in inland waterways. High water levels typically allow for full utilization of vessel capacity, enhancing operational efficiency and profitability, but may introduce clearance issues under bridges, restricting larger vessels. Conversely, low water levels reduce the number of containers that can be transported per trip due to the increased risk of grounding, thereby raising transportation costs. This was evident on the Rhine River in 2018 and 2022, when low

water levels led to an 11.1% decline in freight volumes due to navigational constraints (Destatis , 2019). To address these challenges, we propose a tactical planning framework that explicitly integrates the relationship between water levels and vessel characteristics. Given predicted water levels across the network, the model aims to maximize expected carrier revenue over a tactical horizon (e.g., a season) by establishing a tactical plan detailing the service network, resource utilization, and shipment handling and transport activities for a given schedule length (e.g., a week), executed repeatedly throughout the season. This integration supports adaptive, efficient, and profitable IWT operations under variable waterway conditions.

The remainder of the paper is structured as follows: Section 2 discusses water levels and vessel characteristics; Section 3 presents the mathematical model formulation; Section 4 reports experimental results and analyses; and Section 5 concludes with a summary of findings and directions for future research.

2 Water Levels and vessel characteristics

On one hand, the variability of waterway depth—typically measured at critical points along the waterway as the vertical distance between the water surface and the riverbed or canal bottom—represents a key operational constraint in IWT. Water levels rarely remain constant throughout an entire waterway and often vary from segment to segment due to both natural factors (e.g., geographic location, rainfall, droughts, snowmelt, sedimentation) and human interventions (e.g., dam operations, dredging, or water withdrawals for agricultural and urban use). For instance, upstream dam releases may temporarily raise water levels in certain sections while reducing downstream flow, resulting in shallower segments. Similarly, heavy rainfall can improve navigability, whereas prolonged drought or sediment buildup may decrease it. These variations are typically uneven, meaning that different sections of a river or canal may exhibit significantly different water levels at the same time.

On the other hand, another key operational constraint lies in the physical characteristics of vessels navigating inland waterways. One critical parameter is the vessel's draught—defined as the vertical distance between the waterline and the lowest point of the hull—which indicates how deeply the vessel is submerged and is directly influenced by the weight of the containers being transported. Each vessel has two critical draught thresholds: the maximum draught, representing the depth reached when the vessel is fully loaded, and the minimum draught, corresponding to the depth when it is empty (Prandtstetter et al. , 2023). These values define the vessel's safe loading range, or loading capacity of each vessel, typically measured in weight (tons), volume (TEUs), or both. A vessel's actual draught, which varies with the number and weight of containers, falls within this defined range. As more containers are loaded, the actual draught increases

accordingly, approaching the maximum value. The rate at which this increase occurs is determined by the vessel's load–draught coefficient, which quantifies the sensitivity of the draught to added weight.

Therefore, for safe and efficient operation of scheduled services in inland waterway transportation, it is essential to consider the relationship between water levels and vessel characteristics. At every segment of the service route, the vessel's draught must remain less than or equal to the available water level. This constraint becomes particularly critical during periods of low water levels, as it limits load capacity and increases the risk of grounding. Conversely, when water levels rise, although submerged clearance improves and allows for heavier loads, another constraint emerges. As the water surface elevates, the entire vessel is lifted, decreasing the vertical distance between the vessel's highest point and overhead structures such as bridges. This may restrict the passage of larger vessels with tall superstructures.

These constraints highlight the importance of adaptive tactical planning that accounts for spatial water level variability and vessel characteristics, as they jointly impact transport capacity, service feasibility, and operational reliability. Integrating these factors into tactical planning frameworks is essential for efficient and reliable IWT operations, ultimately contributing to smooth operations of intermodal transportation networks. To simplify the analysis, the current study focuses primarily on submerged clearance rather than bridge clearance. This choice is supported by several key considerations: first, submerged clearance is the predominant navigational constraint, as most inland waterways are not critically restricted by bridge heights; second, declining water levels—driven by climate change and increasing water withdrawals—occur more frequently and have greater operational impact; and third, the modeling approach is conceptually similar for both submerged and bridge clearance. Therefore, focusing on submerged clearance enables a more relevant and streamlined analysis.

3 Notations and mathematical formulation

3.1 Notations

Let us consider a physical network $\mathcal{G}^{\text{ph}} = (\mathcal{N}^{\text{ph}}, \mathcal{A}^{\text{ph}})$, where $\mathcal{N}^{\text{ph}}$ denotes the set of geographical ports, each having a specific berthing capacity Q_η measured in length units, and $\mathcal{A}^{\text{ph}}$ represents the set of physical links. Each physical link $a \in \mathcal{A}^{\text{ph}}$ is characterized by a specific water level p_a at each time period, which is typically represented by a point estimate derived statistically from historical data. This point estimate, often calculated as the mode or average, reflects the most likely water level along each physical link over the planning horizon.

We define the set of shipping demands $\mathcal{K} = \mathcal{K}^{\mathrm{R}} \cup \mathcal{K}^{\mathrm{P}} \cup \mathcal{K}^{\mathrm{F}}$, where $\mathcal{K}^{\mathrm{R}}$ (regular shippers) includes demands that must be fully served, $\mathcal{K}^{\mathrm{P}}$ (partial-spot shippers) includes demands that may be partially met, and $\mathcal{K}^{\mathrm{F}}$ (full-spot shippers) includes demands that can either be fully met or not met at all. Each demand $k \in \mathcal{K}$ is defined by its volume $d(k)$ (in TEUs), origin $O(k)$, destination $D(k)$, release time $\alpha(k)$, and due time $\beta(k)$. The volume is converted to weight using a factor ω. Demands can be standard or express ($class(k)$), with express deliveries being charged higher fares ($\phi(k)$). Container type $\gamma(k) \in \Gamma$ influences handling, storage, and transportation costs.

Let $\mathcal{V}$ denote the set of vessel types, and let F_v represent the maximum number of vessels of type $v \in \mathcal{V}$ available. Each vessel $v \in \mathcal{V}$, pre-assigned to a service, follows a circular sequence of services, starting and ending at the same port. Vessels are characterized by their nominal speed and nominal capacity, measured as $\mathrm{cap}_w(v)$ in tonnage and $\mathrm{cap}_{vol}(v)$ in TEUs. Additional characteristics include length $\mathrm{len}(v)$, maximum draught $dh^+(v)$, minimum draught $dh^-(v)$ and the load-draught coefficient $\theta(v)$, measured in meters per tonnage, which quantifies how changes in loaded weight affect the vessel's draught. The set of potential services the carrier may operate to meet transportation demand is denoted by Σ. Each potential service $\sigma \in \Sigma$ is defined by its route in the physical network and by its schedule. The route of a potential service σ is specified as an ordered set of consecutive stops, including the origin, destination, and intermediate stops, denoted as $\mathcal{N}^{\mathrm{ph}}(\sigma) = \{\eta_i(\sigma) \mid i = 0, \ldots, n(\sigma)\}$. Here, $n(\sigma) = |\mathcal{N}^{\mathrm{ph}}(\sigma)| - 1$ and i indicates the i^{th} stop of the service, with $\eta_0(\sigma) = O(\sigma)$ and $\eta_n(\sigma) = D(\sigma)$ as the origin and destination of the service, respectively. These services are characterized by schedules that specify the departure and arrival times, $\alpha(\eta_i(\sigma))$ and $\beta(\eta_i(\sigma))$, respectively, at each terminal $\eta_i(\sigma)$ in $\mathcal{N}^{\mathrm{ph}}(\sigma)$. Each service has a total duration $\delta(\sigma)$, which includes the time spent at each stop as well as the travel time for each leg. A leg $l_i(\sigma)$ is defined as the segment between each pair of consecutive stops and is expressed as $(\eta_{i-1}(\sigma), \eta_i(\sigma))$ for $i = 1, \ldots, n(\sigma)$. Network operating costs include holding costs ($h(\eta, v)$) for idle vessels at terminals, fixed service setup costs ($f(\sigma)$), and penalties ($\mu(v)$) for unused vessels. Demand fulfillment costs cover transportation, holding, and handling. Transportation costs depend on container type and vessel type ($c_i(\gamma(k), v(\sigma))$), terminal storage costs are represented by $c(\eta, \gamma(k))$, and handling costs by $\kappa(\eta_i(\sigma), \gamma(k))$.

3.2 Mathematical formulation

The SSND-RRM problem is formulated on a time-space network $\mathcal{G} = (\mathcal{N}, \mathcal{A})$. This network is based on time discretization over the schedule length T, divided into equal-length time periods, $t \in \{0, 1, \ldots, T-1\}$. The node set $\mathcal{N}$ is defined as $\{(\eta, t) \mid \eta \in \mathcal{N}^{\mathrm{ph}}, t = 0, \ldots, T-1\}$, representing all terminals in the physical network at each time instant. The arc set $\mathcal{A}$ is the union of moving arcs and holding arcs, $\mathcal{A} = \mathcal{A}^M \cup \mathcal{A}^H$. The set $\mathcal{A}^M$ represents movements between nodes and is defined as: $\mathcal{A}^M = \{((\eta, t), (\eta', t')) \mid \eta, \eta' \in \mathcal{N}^{\mathrm{ph}}, t, t' \in \{0, \ldots, T-1\}, t < t'\}$. This indicates movements between nodes η

and η', departing at time t and arriving at time t'. The set $\mathcal{A}^H$ is defined as: $\mathcal{A}^H = \{((\eta, t), (\eta, t+1)) \mid \eta \in \mathcal{N}^{\text{ph}}, t \in \{0, \ldots, T-1\}\}$. These represent a one-time period waiting at terminal η at time t for vessels, demand, and services. According to the definition of moving arcs in the time-space network, each service leg corresponds to a moving arc. Specifically, a moving arc standing for service leg $l_i(\sigma) = \{(\eta_{i-1}(\sigma), \eta_i(\sigma)) \mid i = 1, \ldots, n(\sigma), \sigma \in \Sigma\}$, is defined as $a_{l_i(\sigma)} = ((\eta_{i-1}(\sigma), \alpha(\eta_{i-1}(\sigma))), (\eta_i(\sigma), \beta(\eta_i(\sigma)))$. This arc indicates the departure of the service leg from terminal $\eta_{i-1}(\sigma)$ at time $\alpha(\eta_{i-1}(\sigma))$ and its arrival at terminal $\eta_i(\sigma)$ at time $\beta(\eta_i(\sigma))$. The second type of arc referred to as a holding arc, is thus defined as $a_{\eta t} = ((\eta, t), (\eta, t+1))$, where $(\eta, t) \in \mathcal{N}$. As we formulated the problem on a time-space network, the characteristics of nodes and arcs in the physical network are represented in the time-space network. The water levels, which are defined for each physical link over different periods, can be directly mapped onto moving arcs in the time-space network. Specifically, the water level for a physical arc, denoted as p_a, is represented as $p_{a_{l_i(\sigma)}}$for moving arcs $a_{l_i(\sigma)} \in \mathcal{A}^M$. Similarly, the berthing capacity Q_η for nodes is represented as $Q_{a_{\eta t}}$ for holding arcs $a_{\eta t} \in \mathcal{A}^H$. Having established the time-space network, we proceed to formulate the SSND-RRM model by first introducing the decision variables:

- $y(\sigma) \in \{0, 1\}$**:** 1 if transportation service σ is selected, 0 otherwise.
- $\xi(k) \in [0, 1]$**:** percentage of the volume of partial-spot shipper demand $k \in \mathcal{K}^{\text{P}}$ that is selected and will be serviced.
- $\zeta(k) \in \{0, 1\}$**:** 1 if full-spot shipper demand $k \in \mathcal{K}^{\text{F}}$ is serviced, 0 otherwise.
- $z(v, a_{\eta_t}) \in \mathbb{Z}\geq 0$**:** number of temporarily idle vessels of type v waiting at holding arc $a\eta_t$ for the departure of the next service they support.
- $B(v) \in \mathbb{Z}\geq 0$**:** total number of vessels of type v used in the service plan. Due to the circular nature of the schedule, it $B(v)$ remains constant across all time periods, although vessels may either be moving or idle in ports at any given period.
- $x(k, a_{l_i}(\sigma)) \geq 0$**:** volume of demand $k \in \mathcal{K}$ transported by service σ on its i^{th} leg.
- $x^{\text{out}}(k, a_{l_i}(\sigma)) \geq 0$**:** volume of demand $k \in \mathcal{K}$ to be unloaded from leg i of service σ.
- $x^{\text{in}}(k, a_{l_i}(\sigma)) \geq 0$**:** volume of demand $k \in \mathcal{K}$ to be loaded onto leg i of service σ.
- $x^{\text{hold}}(k, a_{\eta_t}) \geq 0$**:** volume of demand $k \in \mathcal{K}$ to be held at terminal η during the time period $(t, t+1)$.

$$\begin{aligned}
&\max \sum_{k\in\mathcal{K}^{\mathrm{R}}} \phi(k)d(k) + \sum_{k\in\mathcal{K}^{\mathrm{P}}} \phi(k)\xi(k)d(k) + \sum_{k\in\mathcal{K}^{\mathrm{F}}} \phi(k)\zeta(k)d(k) \\
&- \sum_{v\in\mathcal{V}} \mu(v)(F_v - B(v)) - \sum_{\sigma\in\Sigma} f(\sigma)y(\sigma) - \sum_{a_{\eta_t}\in\mathcal{A}^H} \sum_{v\in\mathcal{V}} h(\eta, v)z(v, a_{\eta_t}) \\
&- \sum_{a_{l_i}(\sigma)\in\mathcal{A}^M} \sum_{k\in\mathcal{K}} c_i(\gamma(k), v(\sigma))x(k, a_{l_i}(\sigma)) - \sum_{a_{\eta_t}\in\mathcal{A}^H} \sum_{k\in\mathcal{K}} c(\eta, \gamma(k))\mathrm{x}^{\mathrm{hold}}(k, a_{\eta_t}) \\
&- \sum_{a_{l_i}(\sigma)\in\mathcal{A}^M} \sum_{k\in\mathcal{K}} \kappa(\eta_i(\sigma), \gamma(k))(\mathrm{x}^{\mathrm{in}}(k, a_{l_i}(\sigma)) + \mathrm{x}^{\mathrm{out}}(k, a_{l_i}(\sigma)))
\end{aligned} \tag{1}$$

Subject to

$$\mathrm{x}^{\mathrm{hold}}(k, a_{\eta_t}) + \sum_{a_{l_i}(\sigma)\in\mathcal{A}^M, (\eta_{i-1}=\eta, \alpha(\eta_{i-1})=t)} \mathrm{x}^{\mathrm{in}}(k, a_{l_i}(\sigma)) = \begin{cases} d(k), & \forall k \in \mathcal{K}^{\mathrm{R}}, \eta = O(k), t = \alpha(k) \\ \xi(k)d(k), & \forall k \in \mathcal{K}^{\mathrm{P}}, \eta = O(k), t = \alpha(k) \\ \zeta(k)d(k), & \forall k \in \mathcal{K}^{\mathrm{F}}, \eta = O(k), t = \alpha(k) \end{cases} \tag{2}$$

$$\sum_{\alpha(k)<t\leq\beta(k)} \sum_{a_{l_i}(\sigma)\in\mathcal{A}^M, (\eta_i=\eta, \beta(\eta_i)=t)} \mathrm{x}^{\mathrm{out}}(k, a_{l_i}(\sigma)) = \begin{cases} d(k), & \forall k \in \mathcal{K}^{\mathrm{R}}, \eta = D(k), \\ \xi(k)d(k), & \forall k \in \mathcal{K}^{\mathrm{P}}, \eta = D(k) \\ \zeta(k)d(k), & \forall k \in \mathcal{K}^{\mathrm{F}}, \eta = D(k) \end{cases} \tag{3}$$

$$\begin{aligned}
&\mathrm{x}^{\mathrm{hold}}(k, a_{\eta_{t-1}}) + \sum_{a_{l_i}(\sigma)\in\mathcal{A}^M(\eta_i=\eta, \beta(\eta_i)=t)} \mathrm{x}^{\mathrm{out}}(k, a_{l_i}(\sigma)) \\
&-\mathrm{x}^{\mathrm{hold}}(k, a_{\eta_t}) - \sum_{a_{l_i}(\sigma)\in\mathcal{A}^M((\eta_{i-1}=\eta, \alpha(\eta_{i-1})=t)} \mathrm{x}^{\mathrm{in}}(k, a_{l_i}(\sigma)) = 0 \\
&\forall (\eta, t) \neq (O(k), \alpha(k)) \forall \eta \neq D(k), \forall k \in \mathcal{K}
\end{aligned} \tag{4}$$

$$\mathrm{x}^{\mathrm{in}}(k, a_{l_i}(\sigma)) - x(k, a_{l_i}(\sigma)) = 0, \forall a_{l_i}(\sigma) \in \mathcal{A}^M,\ \eta_{i-1}(\sigma) = O(\sigma),\ k \in \mathcal{K} \tag{5}$$

$$x(k, a_{l_i}(\sigma)) - \mathrm{x}^{\mathrm{out}}(k, a_{l_i}(\sigma)) = 0, \forall a_{l_i}(\sigma) \in \mathcal{A}^M,\ \eta_i(\sigma) = D(\sigma),\ k \in \mathcal{K} \tag{6}$$

$$\begin{aligned}
&x(k, a_{l_{i-1}}(\sigma)) - \mathrm{x}^{\mathrm{out}}(k, a_{l_{i-1}}(\sigma)) + \mathrm{x}^{\mathrm{in}}(k, a_{l_i}(\sigma)) - x(k, a_{l_i}(\sigma)) = 0, \\
&\forall \sigma \in \Sigma,\ \eta_{i-1} \neq O(\sigma), \eta_i \neq D(\sigma),\ k \in \mathcal{K}
\end{aligned} \tag{7}$$

$$\omega \sum_{k \in \mathcal{K}} x(k, a_{l_i}(\sigma)) \leq cap_w(v(\sigma))y(\sigma), \quad \forall \sigma \in \Sigma, a_{l_i}(\sigma) \in \mathcal{A}^M \tag{8}$$

$$\sum_{k \in \mathcal{K}} x(k, a_{l_i}(\sigma)) \leq cap_{vol}(v(\sigma))y(\sigma), \quad \forall \sigma \in \Sigma, a_{l_i}(\sigma) \in \mathcal{A}^M \tag{9}$$

$$\theta(v(\sigma))\omega \sum_{k \in \mathcal{K}} x(k, a_{l_i}(\sigma)) + dh^-(v(\sigma)) \leq p_{a_{l_i}(\sigma)} \quad \forall \sigma \in \Sigma, a_{l_i}(\sigma) \in \mathcal{A}^M \tag{10}$$

$$B(v) = \sum_{\eta \in \mathcal{N}^{\text{ph}}} z(v, a_{\eta_0}) + \sum_{\sigma \in \Lambda_{0l}} y(\sigma), \quad \forall v \in \mathcal{V} \tag{11}$$

$$B(v) \leq F_v, \quad \forall v \in \mathcal{V} \tag{12}$$

$$\sum_{\sigma \in \Sigma^-_{\eta t v}} y(\sigma) + z(v, a_{\eta_{t-1}}) = \sum_{\sigma \in \Sigma^+_{\eta t v}} y(\sigma) + z(v, a_{\eta_t}) \quad \forall v \in \mathcal{V}, \ a_{\eta_{t-1}}, a_{\eta_t} \in \mathcal{A}^H \tag{13}$$

$$\sum_{v \in \mathcal{V}} len(v)(\sum_{\sigma \in \Sigma^-_{\eta t v}} y_\sigma + z(v, a_{\eta_{t-1}})) \leq Q_{a_{\eta t}}, \quad \forall a_{\eta t} \in \mathcal{A}^H \tag{14}$$

$$y(\sigma) \in \{0, 1\} \quad \forall \sigma \in \Sigma \tag{15}$$

$$\xi(k) \in [0, 1] \quad \forall k \in \mathcal{K}^{\text{P}} \tag{16}$$

$$\zeta(k) \in \{0, 1\} \forall k \in \mathcal{K}^{\text{F}} \tag{17}$$

$$z(v, a_{\eta_t}) \geq 0 \quad \forall v \in \mathcal{V}, \quad a_{\eta_t} \in \mathcal{A}^H \tag{18}$$

$$B(v) \geq 0, \text{integer} \quad \forall v \in \mathcal{V} \tag{19}$$

$$x(k, a_{l_i}(\sigma)) \geq 0 \quad \forall k \in \mathcal{K}, \ a_{l_i}(\sigma) \in \mathcal{A}^M \tag{20}$$

$$\text{x}^{\text{out}}(k, a_{l_i}(\sigma)) \geq 0 \quad \forall k \in \mathcal{K}, \ a_{l_i}(\sigma) \in \mathcal{A}^M \tag{21}$$

$$\text{x}^{\text{in}}(k, a_{l_i}(\sigma)) \geq 0 \quad \forall k \in \mathcal{K}, \ a_{l_i}(\sigma) \in \mathcal{A}^M \tag{22}$$

$$\text{x}^{\text{hold}}(k, a_{\eta_t}) \geq 0 \quad \forall k \in \mathcal{K}, \ a_{\eta_t} \in \mathcal{A}^H. \tag{23}$$

The objective function (1) maximizes net profit by considering revenue from servicing regular, partial-spot, and full-spot shippers, along with costs related to unused vessels, service setup, vessel idling, container transportation, and handling at terminals. Equations (2), (3), and (4) are flow-conservation constraints for containers of all shipper types, at their particular origins, destinations, and intermediary nodes, respectively. Similarly, Equations (5), (6) and (7) enforce the conservation of container flows, for all shipper types, on each service at its origin, destination and intermediary stops, respectively. (8) and (9) guarantee that the weight and volume of all demands $k \in \mathcal{K}$ transported by service σ on its leg i do not exceed the nominal capacity of vessel v performing service σ. Constraint (10) assures that the draught of vessels executing the i^{th} leg of service σ is less than or equal to the water level on that leg. Equation (11) computes the number of vessels used in the plan as the sum of vessels idling in ports or moving between them performing services. Due to the resource management concerns and the resulting circular vessel routes, $B(v)$ is the same at all periods, only the relative proportion of idle versus active vessels being different at different time periods. We therefore compute this number for the first period, i.e., $t = 0$, the set $\Lambda_{0l} = \{\sigma \in \Sigma, v(\sigma) = v | (\alpha_{n(\sigma)} \mod T) < \beta_0(\sigma) \text{ and } \beta_0(\sigma) \geq 0\} \subseteq \Sigma$ containing all services, of the appropriate vessel type, that operate one of its legs during the first period. Constraints (12) enforce the fleet size for each vessel type, while Equations (13) are the so-called design-balance constraints, enforcing the vehicle-flow conservation at terminals (the number of services and idle vessels entering a node equals the number exiting the node), where sets $\Sigma^-_{\eta t v} = \{\sigma \in \Sigma \mid \eta_i(\sigma) = \eta, \beta(\eta_i(\sigma)) = t, v(\sigma) = v, \text{ for } i = 1, \ldots, n(\sigma)\}$ and $\Sigma^+_{\eta t v} = \{\sigma \in \Sigma \mid \eta_i(\sigma) = \eta, \alpha(\eta_i(\sigma)) = t, v(\sigma) = v, \text{ for } i = 0\}$ group the services with a vessel type v that arrive at their destination or depart from their origin, respectively. Finally, Constraints (14) enforce the terminal berthing capacity at each time period. Decision-variable domains are defined by Constraints (15) - (23).

4 Experimental results

We generate test instances for two network topologies: a linear network with four connected terminals and a star network with five terminals linked to a central hub. Water levels are considered at critical points along the waterways, ranging between 150 cm and 350 cm, reflecting natural variations as described by (Christodoulou et al., 2020). The linear and star networks include 20 and 71 routes, respectively. Two types of vessels are used: small and large, with nominal capacities of 20 and 50 TEUs, respectively, and with large vessels costing twice as much as small vessels. Services are scheduled with nine distinct start times over a 14-period weekly cycle, resulting in 360 potential services for the linear network (20 routes $\times$ 9 start times $\times$ 2 vessel types) and 1278 for the star network (71 routes $\times$ 9 start times $\times$ 2 vessel types). Four demand instances are generated for each network, with demand volumes randomly ranging between 5 and 25 TEUs. The naming convention for test instances comprises two parts: the first part

specifies the network topology, where "L" denotes the linear network and "S" denotes the star network. The second part indicates the number of demand requests, ensuring a diverse range of transportation needs. In the following, we present the analysis and results obtained using the described test instances. All implementations were carried out using the Pyomo software package and the Gurobi solver on a machine equipped with an Intel(R) Xeon(R) CPU E5-2630 v4 @ 2.20GHz and 256GB of memory. The results from the computational experiments, summarized in Tables 1 to 4, compare solutions with and without water level constraints for both linear and star networks. Tables 1 and 2 show results for the linear network, while Tables 3 and 4 present results for the star network. Performance indicators such as profitability, service costs, demand flow costs, capacity utilization (measured as the ratio of total volume-kilometers moved to total capacity-kilometers operated), and shipper satisfaction (the proportion of requested demand volume accepted for transportation) are evaluated.

In terms of profitability, excluding water level constraints consistently yields higher results. In the linear network, the impact is especially pronounced. For instance, profit increases from 184,827.84 to 222,641.00 in TestL-124, and from 191,580.54 to 230,475.00 in TestL-136. On average, the linear network sees a 20.4% increase in profitability when water levels are not considered. In the star network, the gain is more modest, with an average increase of approximately 0.5%. The most significant improvement occurs in TestS-170, where profit increases from 272,659.51 to 273,399.00 units.

Table 1: Performance Evaluation of Solutions with Water Levels for Linear Network

Test Name	Profit	Demand Flow Cost	Service Cost	Shipper Satisfaction (%)	Capacity Usage (%)
TestL-73	109,523.79	31,426.21	2,240.00	57.32	59.27
TestL-89	136,297.30	36,442.81	3,080.00	53.52	45.56
TestL-124	184,827.84	45,461.85	3,220.00	37.61	48.23
TestL-136	191,580.54	51,029.85	3,080.00	41.57	56.63

Table 2: Performance Evaluation of Solutions without Water Levels for Linear Network

Test Name	Profit	Demand Flow Cost	Service Cost	Shipper Satisfaction (%)	Capacity Usage (%)
TestL-73	110,318.00	30,402.00	2,170.00	61.02	58.29
TestL-89	150,407.00	40,543.00	2,940.00	63.41	53.62
TestL-124	222,641.00	56,074.00	3,570.00	68.81	61.42
TestL-136	230,475.00	63,030.00	3,780.00	64.07	57.67

When water level constraints are considered, service costs tend to increase due to a higher number of services and greater reliance on small vessels. Given their lower nominal capacity compared to large vessels, small vessels offer fewer consolidation opportunities, resulting in limited cost savings. This effect is observed in TestL-73 and TestL-89, where service costs are higher under water level constraints (2,240.00 vs. 2,170.00; 3,080.00 vs. 2,940.00), along with an increase in the number of services and the share of small vessels. Specifically, TestL-73 involves 30 services (2 large, 28 small) compared to 23 services (8 large, 15 small) when water level constraints are not considered. Similarly, in TestL-89, the fleet composition shifts from 8 large and 28 small vessels to 12 large and 18 small.

When water level constraints are not considered, the total number of services generally decreases and the share of large vessels increases, enhancing consolidation opportunities and allowing for greater potential cost savings. However, in some cases, such as TestL-124 and TestL-136, the increased use of large vessels results in higher fixed costs, which are not fully compensated by the consolidation gains. As a result, total service costs increase—from 3,220.00 to 3,570.00 in TestL-124, and from 3,080.00 to 3,780.00 in TestL-136. In TestL-124, the number of large vessels increases from 8 (with constraints) to 25 (without), while small vessels decrease from 30 to 1. Similarly, in TestL-136, the fleet shifts from 8 large and 28 small vessels to 23 large and 8 small vessels. A similar

Table 3: Performance Evaluation of Solutions with Water Levels for Star Network

Test Name	Profit	Demand Flow Cost	Service Cost	Shipper Satisfaction (%)	Capacity Usage (%)
TestS-127	183,972.38	77,457.62	2,170.00	24.95	40.17
TestS-142	206,095.10	83,814.90	2,590.00	24.82	35.70
TestS-170	272,659.51	105,167.53	2,170.00	18.76	41.39
TestS-228	329,126.75	134,933.25	2,940.00	20.95	43.34

Table 4: Performance Evaluation of Solutions without Water Levels for Star Network

Test Name	Profit	Demand Flow Cost	Service Cost	Shipper Satisfaction (%)	Capacity Usage (%)
TestS-127	184,194.00	77,446.00	1,960.00	23.70	39.91
TestS-142	207,722.00	84,368.00	2,310.00	25.99	43.55
TestS-170	273,399.00	105,016.00	2,380.00	22.62	47.05
TestS-228	329,330.00	134,690.00	3,080.00	24.41	46.96

pattern is observed in the star network. When water levels are considered, more services are activated to compensate for the reduced vessel capacity. For example, in TestS-127, the system operates 5 large and 21 small vessels (total: 26), compared to 4 large and 20 small (total: 24) without water level constraints. In TestS-142, the fleet decreases from 29 vessels (8 large and 21 small) to 27 (6 large and 21 small) when constraints are removed, resulting in a reduction in service cost—from 2,590.00 (with water levels) to 2,310.00 (without). However, in TestS-170 and TestS-228, service costs increase when water level constraints are removed. In TestS-170, the cost rises from 2,170.00 (with water levels) to 2,380.00 (without), and in TestS-228, from 2,940.00 to 3,080.00. This increase occurs despite the total number of services remaining constant (28 in both cases), as the system shifts toward a greater reliance on large vessels in the absence of navigational limitations. Therefore, water level constraints impact service costs by influencing both the number of services operated and the types of vessels deployed, depending on demand levels and navigability.

Demand flow costs generally decrease when water level constraints are applied, but this reduction reflects unmet demand rather than improved efficiency. In the linear network, demand flow costs drop significantly (e.g., TestL-89: 40,543.00 to 36,442.81), but lower capacity usage and decreased shipper satisfaction indicate poor utilization of vessel capacity. For instance, shipper satisfaction drops from 63.41% to 53.52% in TestL-89. Only TestL-73 shows stable performance with a slight cost increase but relatively consistent satisfaction and capacity usage. In the star network, demand flow costs and shipper

satisfaction remain stable with or without water level constraints, suggesting resilience due to the centralized structure where all nodes connect to a central hub. The average demand flow cost is similar (100,343.83 with constraints vs. 100,379.5 without), and satisfaction only slightly varies (22.37% vs. 24.18%), indicating consistent performance despite navigational challenges.

5 Conclusions and perspectives

This study introduces varying water levels as a critical environmental and infrastructural constraint in the tactical planning of consolidation-based inland waterway carriers. By enhancing the existing methodology, we propose a framework that explicitly models the relationship between vessel load capacity and water levels, ensuring service feasibility only when a vessel's draught remains less than or equal to the available water level.

Experimental tests illustrate that the proposed model offers a more accurate and resilient approach to service network design, resource utilization, and demand satisfaction. Comparative analysis across linear and star network topologies shows that neglecting water level constraints leads to overestimated profitability and shipper satisfaction. Incorporating water levels encourages the use of smaller, adaptable vessels, increased service selection, and capacity deployment adjustments aligned with actual navigability conditions. Additionally, the analysis reveals that linear networks are more vulnerable to water level fluctuations due to limited routing options, where each node is directly connected only to its neighbors. In contrast, star networks benefit from a centralized structure that provides multiple routing alternatives through a central hub, enhancing flexibility and robustness against disruptions.

Future research could improve the model by incorporating stochastic water levels, addressing uncertainties in environmental and infrastructure conditions, and considering how water levels affect service travel times, including delays and associated penalty costs for late pickups and deliveries. This enhancement would provide more realistic insights and support better decision-making in inland waterway freight transportation.

Acknowledgements

While working on the project, the first author was a Ph.D. candidate at the School of Management, Université du Québec à Montréal (UQAM), Canada, and a member of CIRRELT. The third author held the UQAM Chair in Intelligent Logistics and Transportation Systems Planning, and was an Adjunct Professor in the Department of Computer

Science and Operations Research at the Université de Montréal, while the fourth author held the Canada Research Chair in Stochastic Optimization of Transport and Logistics Systems. We gratefully acknowledge the financial support provided by the Natural Sciences and Engineering Research Council of Canada (NSERC), through its Collaborative Research and Development, and Discovery grant programs. We also gratefully acknowledge the support of Fonds de recherche du Québec through their infrastructure grants. Finally, during the preparation of this work the authors used ChatGPT-4, under its most strict privacy enforcing settings, for text edit purposes exclusively. After using this tool, the authors reviewed and further edited the text as needed and take full responsibility for the content of the publication.

References

CEIC Data., 2023. United States inland waterways freight transport, total.

European Commission, Eurostat., 2023. Freight transport statistics - modal split.

Bilegan, I. C., Crainic, T. G., Wang, Y., 2022. Scheduled service network design with revenue management considerations and an intermodal barge transportation illustration. European Journal of Operational Research 300(1), 164–177.

Federal Statistical Office of Germany (Destatis)., 2019. Freight transport on German inland waterways decreased by 11.1% in 2018. Wiesbaden.

Prandtstetter, M., Widhalm, P., Leitner, H., Czege, I., 2023. A novel visualisation tool for reliable inland navigation. Transportation Research Procedia 72, 3537–3544.

Christodoulou, A., Christidis, P., Bisselink, B. (2020). Forecasting the impacts of climate change on inland waterways. Transportation Research Part D: Transport and Environment 82, 102159.

Appendix

For this study, the scheduling horizon is a one-week period (7 days), divided into 14 half-day intervals, reflecting standard inland waterway transportation practices where departures and arrivals typically occur in morning and afternoon slots. This section provides an overview of the test instances, covering the network topology, potential services and their schedules, and demand data.

Physical network and its relevant features. We generate a set of test instances based on two distinct physical network topologies, as shown in Figures 1 and 2. The first is a linear network with four sequentially connected terminals, while the second is a star network comprising six terminals. The linear topology is inspired by existing European networks due to its relevance, representing a typical corridor structure found in regions such as northern France and Belgium. In contrast, the star network represents a more complex inland waterway system, where all terminals are connected to a central hub. One key infrastructure limitation is terminal capacity. For each network topology, berthing capacities at terminals are randomly assigned, ranging from 700 meters to 1000 meters, ensuring the simultaneous berthing of multiple vessels based on predefined vessel sizes.The cost structure associated with terminal operations is considered as follows: the loading and unloading of containers incur a cost of 2 units per operation, terminal activities such as storage are charged to carriers at a rate of 3 units per container per period, and vessel holding costs at terminals are set at 5 units per period. Additionally, we consider water levels at critical points along the waterways. The range of water levels is based on the study by (Christodoulou et al., 2020), spanning randomly between 150 cm and 350 cm, reflecting the natural variations in inland waterway conditions.

Service network generation. Potential services are designed for both the linear and star network topologies, covering 20 and 71 routes, respectively. Services are scheduled to commence at various times throughout the 14-period weekly cycle, ensuring operational flexibility. Among these, nine distinct start times are selected to maintain a diverse and well-distributed schedule. Based on this scheduling structure, the total number of potential services is calculated by multiplying the number of routes by the number of start times, resulting in 180 services for the linear network and 639 services for the star network. Each of these services can be operated using either a large or small vessel, effectively doubling the total number of services to 360 for the linear network and 1278 for the star network. The duration of each service is determined by considering both travel time between terminals and time spent at the origin, destination, and intermediate stops, where each stop is assumed to require one time period. Travel times between terminals are defined proportionally to the distance between them, with adjacent terminals having the shortest travel times. As the distance increases, travel times increase accordingly. Large vessels are faster, with travel times half that of small vessels. Dimensions of each vessel type are as follows: Large Vessels: Measuring 200 meters in length, with a minimum draught of 135 centimeters, these vessels support a maximum weight of 500 tons and can

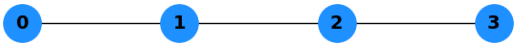

Figure 1: Linear network

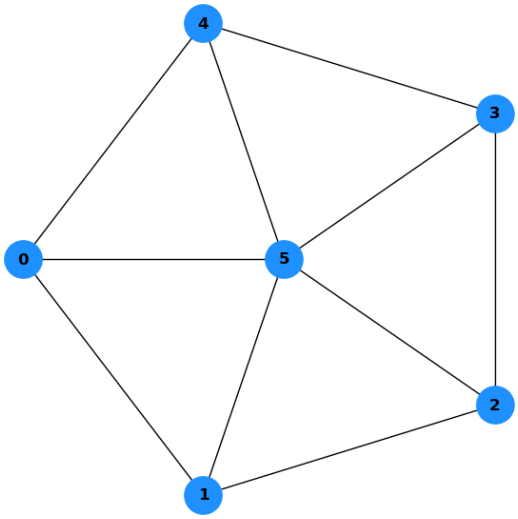

Figure 2: Star network

carry up to 50 TEUs. The draught-weight factor for large vessels is 0.4. Small Vessels: Half the length of large vessels (100 meters), with a minimum draught of 100 centimeters, these vessels can carry up to 200 tons and 20 TEUs. The draught-weight factor for small vessels is 0.3. Operating a large vessel incurs approximately twice the cost of operating a small one, reflecting economies of scale. It is noteworthy that both vessel types are capable of navigating the entire network in both directions when they are empty because the minimum water level is 150 cm.

Demand Generation. We generate four distinct demand instances for the computational experiments to comprehensively evaluate the model's performance. For the linear network, we generate 73, 89, 124, and 136 demand requests, while for the star network, the four demand instances contain 127, 142, 170, and 228 demand requests. For both networks, demand requests are assigned based on randomly selected origin-destination (OD) pairs, ensuring a broad coverage of possible transportation needs. The volume of each demand request is randomly generated between 5 and 25 units. Demand requests consist of three shipper categories: regular, partial spot, and full spot shippers, with each category further classified into express and standard deliveries, where the unit revenue for express deliveries is twice as high as for standard ones. The desired pickup time window is uniformly generated between 1 and 7 periods, while the delivery duration depends on the request type. Express deliveries require 1 to 3 periods, whereas standard deliveries take twice as long as express deliveries for the same origin and destination.